

Electronic and magnetic properties of NiPd and CoPd nanostructures

J. Guevara^{a,b}, A.M. Llois^{b,c}, F. Aguilera-Granja^d, and J.M. Montejano-Carrizales^{d,*}

^aEscuela de Ciencia y Tecnología, Universidad de San Martín, Campus Miguelite - Edificio Tornavias, Martín de Irigoyen 3100, (1650) San Martín, Argentina.

^bDepartamento de Física, CAC-CNEA,

Avda. Gral. Paz 1499, (1650) San Martín, Argentina.

^cDepartamento de Física, FCEyN-UBA,

Cdad. Universitaria, 1428 Buenos Aires, Argentina,

^dInstituto de Física, Universidad Autónoma de San Luis Potosí,

San Luis Potosí, México,

*e-mail: jmmc@ifisica.uaslp.mx

Recibido el 16 de junio de 2009; aceptado el 13 de enero de 2010

We study the dependence of the magnetic properties of NiPd and CoPd segregated nanoclusters and slabs as a function of the 3d magnetic component concentration (x), the chemical order, and size. In the case of clusters we consider 3d cores coated by Pd atoms (3d/Pd) and also onion-like (Pd/3d/Pd) configurations. For the slabs we consider different possible segregated structures of the 3d and 4d atoms and study the evolution of the magnetic properties on these different configurations. We show that Pd coating gives rise to an enhancement of the average magnetic moment of the Ni or Co core atoms and of the Pd atoms as well. Larger values of the average magnetic moments are obtained in the onion-like structures (Pd/3d/Pd) than in the core/shell (3d/Pd) configuration. We compare with theoretical and experimental results available in the literature.

Keywords: Bimetallic cluster; magnetic properties; nanostructures; work function.

Se estudia la dependencia de las propiedades magnéticas de nanocúmulos segregados y películas de NiPd y CoPd como función de la concentración de la componente magnética 3d (x), del orden químico y del tamaño. En el caso de los cúmulos, se consideran núcleos 3d cubiertos por átomos Pd (3d/Pd) y también configuraciones por capas tipo cebolla (Pd/3d/Pd). Para las películas se consideran diferentes posibles estructuras segregadas de los átomos 3d y 4d y se estudia la evolución de las propiedades magnéticas de las diferentes configuraciones. Se muestra que la cubierta de Pd da lugar a un incremento del momento magnético promedio de los átomos del núcleo de Ni o Co así como de los átomos de Pd también. Se obtienen valores más grandes de los momentos magnéticos promedio en las estructuras por capas (Pd/3d/Pd) que en las configuraciones núcleo/cubierta (3d/Pd). Se compara con resultados experimentales disponibles en la literatura.

Descriptores: Cúmulos bimetalícos; propiedades magnéticas; nanoestructuras; función de trabajo.

PACS: 75.75.+a; 36.40.Cg; 75.50.-y

Since the bronze age, alloying two or more elements has been the traditional way to modify mechanical and electronic properties of materials with the aim of getting novel ones not present in pure bulk systems. Nowadays, in the light of new technologies, a way to modify the properties of pure systems is by going down in dimensionality. However, the procedures that combine both alloying and finite size effects have not been yet widely explored by the scientific community. There are few works in the literature that explore the competition between alloying and finite size effects, among them we can cite the recently reported experimental results on CoRh low dimensional systems [1] and the theoretical calculations for very small CoRh [2–4], CoAg and CoCu aggregates [5–7].

From both the technological as well as the economical point of view, “nano-alloying” can be very useful in reducing costs in the production of active surface nanoparticles made of very expensive metals and for those applications where inner core atoms do not interact with the environment, such interactions being limited to the surface. For instance, Pd is an expensive and widely used element in catalytic processes

and frequently appears in its low dimensional manifestations (clusters, small particles, wires, deposited films, etc). In order to lower costs, different possibilities have been proposed where the active Pd component constitutes only a small fraction of the particles used for catalytic purposes. The suggested systems are mainly core/coated arrangements which can be used instead of pure Pd particles. A system like Ni (core) coated by Pd has already been synthesized; it preserves the original surface properties, and shows additional ones, such as core induced magnetism. The magnetic properties of these core/coated particles can also be modified by changing core atoms for a harder magnetic material such as Fe or Co [8, 9].

The driving forces that yield to the final chemical order depend on several parameters such as relative atom sizes and surface energies, and also on the tendency of the constituting elements to form compounds at different concentrations [10, 11]. It obviously depends on fabrication processes and *a posteriori* thermal or chemical treatments. Another way of reducing dimensionality is by growing thin films. In

this case confinement is only in one direction and it is worth comparing differences between alloying effects and dimensionality.

Ab initio calculations are limited up to now to small particle sizes, even for highly symmetric structures. In this contribution we use a tight-binding Hamiltonian solved within the unrestricted Hartree-Fock approximation. By taking advantage of symmetry properties, we are able to handle clusters of up to 561 atoms, a size which is already within the real nanoscale of the experimentally produced clusters [1,8,9,12]. In the particular case of Ni and Pd, both are fcc in bulk; they have the same number of valence electrons, but do not form compounds, Ni is much smaller than Pd, and has a larger surface energy [13]. This allows us to assume that NiPd clusters should mainly show a core/coated cluster-like structure, with Ni in the core and Pd at the surface. A similar situation is expected for CoPd clusters. But it has been shown that cluster properties depend on structure, and cluster structures depend on the number of atoms and on the element under consideration. In the case of icosahedral clusters, core/shell structures have been established as the most stable ones. In the case of fcc clusters, onion-shell structures show up competing in energy with core/shell ones [14]. These onion-like structures have in the intermediate shell one kind of element (Ni or Co in our case) and in the core and coating shell the other one (A/B/A structures).

We do not consider spin-orbit coupling in our calculations as it has been shown by Villaseñor-González *et al.* [15] that the contribution of the orbital magnetic moment to the total one can be considered negligible or constant (quenched) for cluster sizes larger than 100 atoms.

We study then the electronic properties of NiPd and CoPd clusters (in the core/coating shell and A/B/A onion-like structures) and finite slabs with different atomic distributions. We assume that the clusters have cubo-octahedral structure and, in particular, we study the dependence of the average magnetic moment, μ , as a function of Ni- or Co-concentration. In the case of thin films, we study the dependence of the mag-

netic properties, total energies, and work function on the different arrangements by doing slab calculations. We compare our results with several *ab-initio* results [16] for clusters and with experiments [8,9].

1. Method of calculation and structures

For the study of NiPd and CoPd nanoclusters and slabs, we use a tight-binding Hamiltonian with *spd* orbitals and parameters from the corresponding bulk materials is used. Only nearest neighbor two center parameters are considered. Magnetism is obtained from a Hubbard-like term solved in the unrestricted Hartree-Fock approximation. All many-body contributions appear in the diagonal term [17]. The single-site energies ϵ_m^0 and the hopping elements of the Hamiltonian are taken from Andersen's canonical LMTO-ASA paramagnetic bands [18]. $U_{mm'}$ are the screened intrasite Coulomb integrals in the solid, the values U_{dd} are obtained using bulk occupations following Ref. 19 and the U_{ss}/U_{dd} relations are taken from atomic tables. $J_{mm'}$ are the intrasite exchange integrals and are assumed to be zero except for *d* orbitals. J_{dd} is fitted, in the case of Ni and Co, to obtain experimental bulk magnetization, without orbital contribution, ($\mu_{Ni}=0.6\mu_B$ and $\mu_{Co}=1.53\mu_B$). For Pd, the exchange interaction $J_{dd} = 0.68$ eV is taken from Ref. 20. The Madelung term, $\Delta\epsilon_i^{MAD}$, is necessary due to the presence of charge transfers among shells within the clusters [17].

Transition metal surfaces show two characteristic features: electron spillover and *d*-orbital occupations almost unchanged with respect to the bulk values. It has been previously shown [17] that both effects can be taken properly into account by adding extra orbitals with *s* symmetry (*s'* orbitals) outside the surface. These extra *s'* orbitals localized in pseudo-atomic sites outside the cluster have been parametrized in order to obtain adequate *d* orbital occupations. The number of *s'* orbitals added is such that the coordination of each surface atom resembles the bulk coordination. All parameters used are listed in Table I.

TABLE I. Tight-binding parameters used in this work taken from Refs. 18 and 19. All the parameters are in eV. The two site integrals are listed from the second to the fourth column. ϵ_m^0 is the site energy of the *m* orbital, $U_{mm'}$ the intrasite Coulomb integrals between orbitals *m* and *m'*, and J_{dd} the exchange integral among *d* orbitals.

	Ni	Co	Pd		Ni	Co	Pd
<i>ssσ</i>	-1.064	-1.065	-0.883	ϵ_s^0	1.663	2.143	0.390
<i>ppσ</i>	1.878	1.869	1.394	ϵ_p^0	6.646	6.938	4.275
<i>ppπ</i>	-0.235	-0.234	-0.174	ϵ_d^0	-3.065	-2.592	-4.465
<i>ddσ</i>	-0.555	-0.630	-0.769	$\epsilon_{s'}^0$	3.012	4.080	0.390
<i>ddπ</i>	0.237	0.270	0.329				
<i>ddδ</i>	-0.022	-0.025	-0.030	U_{ss}	1.20	1.16	1.56
<i>spσ</i>	1.408	1.405	1.105	U_{sd}	1.44	1.40	1.87
<i>sdσ</i>	-0.739	-0.788	-0.793	U_{dd}	3.29	3.06	2.54
<i>pdσ</i>	-0.998	-1.061	-1.012	J_{dd}	1.00	1.20	0.68
<i>pdπ</i>	0.238	0.253	0.241				

The Hamiltonian is solved self-consistently diagonalizing at each step the spin-up and spin-down matrices, and the electronic occupation for each atom, orbital and spin is obtained. In order to define the Fermi level and the occupations, states are considered degenerate if their energies lie within 0.01 eV or less, independently of their spin. These degenerate states are assumed to be equally filled, leading sometimes to a fractional occupation of the highest occupied states.

In the case of clusters, we assume fcc structures with two symmetries:

- i) the cubo-octahedral symmetry for $N = 147, 309,$ and $561,$ whose cores have $55, 147,$ and $309,$ respectively, and
- ii) the truncated octahedral symmetry for $N = 405$ with cores of 201 atoms, with different concentrations of the $3d$ magnetic component.

Each shell of the clusters has one type of atom (Ni, Co, or Pd) in order to take advantage of symmetry properties and to reduce the number of nonequivalent atoms within the clusters. In Fig. 1 we show schematically the structure of 405 and 561 atom clusters. Figure 1a corresponds to the 405 atom cluster, which is a truncated octahedron having 6 squared (100) faces and 8 hexagonal (111) ones. It has 201 atoms with bulk coordination 12 and 204 surface atoms. Figure 1d corresponds to a 561 atom cluster with cubo-octahedral symmetry which has also 6 squared (100) faces but 8 triangular (111) faces. It has 309 atoms with bulk coordination 12 and 252 surface atoms.

We are aware that the core-shell and the onion-like structures may not be the lowest energy structures for these binary alloys; our calculations study the magnetic behavior when such structures are present in the system, and we considered these cases due to the fact that we also present results for binary superlattices.

We consider bulk-like parameters for the homo-atomic interatomic distances and hopping integrals, whereas the average values for the interatomic distances and hopping integrals are used for hetero-atomic interaction. These average values for the hetero-atomic parameters allow us to partially consider the effects coming from the different concentrations in our binary clusters. We consider only two different kinds of configurations in the cluster calculations, the core/coated structures (Ni- or Co-core coated by Pd) and the onion-like A/B/A ones having an intermediate shell of $3d$ (Ni or Co) with the core and coating made of Pd (that is Pd/ $3d$ /Pd). These arrays are illustrated in Fig. 1 for the truncated octahedron [cubo-octahedron] the core/shell in Fig. 1b [1e] and the onion-like in Fig. 1c [1f]. In the case of the core/coated configuration, the $3d$ core grows in steps of complete core closed sub-shells, keeping in this way a highly symmetric structure while increasing the concentration of the magnetic component. For the onion-like arrangement, we consider an A/B/A array (Pd core/ Ni or Co close shell subsurfaces/ Pd external surface). These onion-like configurations have been suggested to be present in some fcc bimetallic

Pd nanoparticles by Baletto and coworkers [14]. For these onion-like arrangements, we restrict ourselves to a 561 atom cluster with fcc cubo-octahedral structure and fixed number of Pd atoms at the surface (252 atoms). This structure shows a core of 309 atoms and a surface region of 252 atoms. The onion-like Pd/ $3d$ /Pd structures can be depicted by Pd $_{309-N}$ / $3d_N$ /Pd $_{252}$ with N going from 60 to 309 . The particular case of $N = 309$ corresponds to the $3d$ -core/coated configuration $3d_{309}$ Pd $_{252}$ described above. We only show the results for Pd $_{309-N}$ /Ni $_N$ /Pd $_{252}$ and Pd $_{309-N}$ /Co $_N$ /Pd $_{252}$. We select this size to compare with experimental results available in the literature [8,9].

The slab calculations are done by using the all-electron full potential *ab initio* Wien2k code [21]. We calculate the electronic and magnetic structure of 7 layer slabs whose lattice parameters depend linearly on concentration, and we use the *ab initio* Ni (Pd) bulk equilibrium lattice constant for the pure Ni (Pd) slab (being 6.45 a.u. for Ni and 7.30 a.u. for Pd). We consider an APW basis and 30 K-points in the irreducible Brillouin zone (400 K-point in the whole zone) and the LDA to DFT for the exchange-correlation potential. The cutoff parameter that gives the number of plane waves in the interstitial region is taken as $R_{\text{mt}}K_{\text{max}} = 7,$ K_{max} being the maximum value of the reciprocal lattice vector used in the expansion of plane waves in that zone. All the slabs are grown in the $(111), (110),$ and (100) directions, each layer having only one type of atom and preserving the reflexion symmetry with respect to the xy -plane. The slab Work Function (WF) is calculated as the difference between the Fermi energy level and the value of the electrostatic potential in the middle of the vacuum region. In all cases the charge is converged up to $10^{-4}e.$

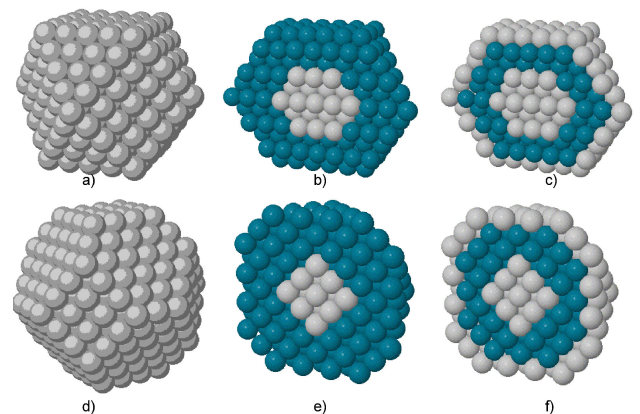


FIGURE 1. Structures of the clusters and the two arrays used here. a) The 405 atom truncated octahedron cluster and d) the 561 atom cubo-octahedron one. b) and e) correspond to the core(gray)/shell(black) array and c) and f) to the onion-like one (inner core in gray, intermediate shell in black, and surface atoms in gray) for the cubo-octahedron and the truncated octahedron, respectively.

2. Results and discussions

Before discussing the trends obtained in the cluster calculations, we compare our results with those corresponding to the *ab-initio* ones performed by Wang *et al.* [16] for some selected core(Ni)/coated(Pd) clusters with a fixed size of $N = 43$, bulk distances for both components, and cubo-octahedral growth structure. In the case of Pd_{43} , our calculated average magnetic moment is $0.046\mu_B$ whereas Wang's is half ours. In both calculations the surface atoms are the ones that show magnetic behavior, whereas the core sites are mainly non-magnetic. For NiPd_{42} our local Ni moment is $1.14\mu_B$, in good agreement with Wang's calculations, and the experimental values are $0.9\mu_B \pm 0.2\mu_B$ as measured by Aldred, [22] and $1.0\mu_B$ and $0.92\mu_B$ as obtained by Loram and Oswald [23, 24], respectively. For $\text{Ni}_{13}\text{Pd}_{30}$ our calculations and Wang's are very similar, whereas for $\text{Ni}_{19}\text{Pd}_{24}$ we obtain $0.51\mu_B$ for the average magnetic moment which is smaller than Wang's ($0.72\mu_B$); finally, for Ni_{43} our calculation gives $0.65\mu_B$ while Wang's is twice as large as our value. In general our values for the Ni magnetic moments are smaller than those obtained by Wang. However both calculations show similar tendencies, that is, a monotonous increasing dependence of the average magnetic moment as a function of Ni concentration. From the previous comparison we have confidence that our calculations are able to describe the general trends.

2.1. Core/shell Clusters' calculations

We calculate the magnetic properties of NiPd and CoPd clusters in the core/shell configurations for different sizes and variable Ni and Co concentration starting in the dilute limit and ending in the pure Ni and Co regimes.

In Fig. 2, we show the results obtained for the average magnetic moment per atom as a function of Ni content (N_{Ni}) for clusters of 405 and 561 atoms. For a fixed total number of atoms, we increase the size of the Ni core (decreasing the number of Pd atoms). Similar behaviors are obtained for the two different cluster sizes and, as expected, the dependence of the magnetic moments on the number of atoms becomes smoother as the cluster size increases. In each case the upper nearly-constant curve gives the average magnetic moment per Ni atom as a function of Ni content, the lower curve gives the corresponding values for Pd, while the one in between (open squares) gives the total average magnetic moment per atom of the system. The enhancement of the magnetic moment of the Ni atoms, as compared to the bulk value, is due to finite size effects and also to hybridization with Pd. The average magnetic moment per Ni atom tends towards the free standing cluster value as a function of increasing Ni concentration for the cluster sizes considered, with $\mu_{\text{Ni}_{561}} = 0.63\mu_B$, in agreement with the experimental reports $(0.62 \pm 0.05)\mu_B$ [26] and $(0.71 \pm 0.02)\mu_B$ [27].

The evolution of the average magnetic moment of the Ni atoms in the two cases shown in Fig. 2 can be explained as

follows. When the number of Ni atoms in the core cluster is less than half the total number of atoms (none of the Ni atoms sits at surface shells), the enhancement is due to hybridization with Pd. For small clusters [Fig. 2a], Pd atoms are polarized, due to both the small cluster size and to the hybridization with Ni. This feedback gives rise to large Ni magnetic moment values. With a growing Ni core (keeping cluster size fixed), only surface effects become important and μ tends to the corresponding free-standing Ni cluster value. At a given concentration, the larger the cluster the smaller the relative number of Ni-Pd bonds over the total number of bonds. This fact limits hybridization effects leading to a vanishing enhancement of the average magnetic moment.

The results of our cluster calculations are in good qualitative agreement with the experimental results by Nuno-mura [9] for NiPd particles of around 562 atoms. The dependence of the magnetic moment on Ni concentration, as in Fig. 2, describes similar tendencies for both curves. Our cluster calculations are performed for completely segregated cubo-octahedral systems, while in Ref. 9 no experimental

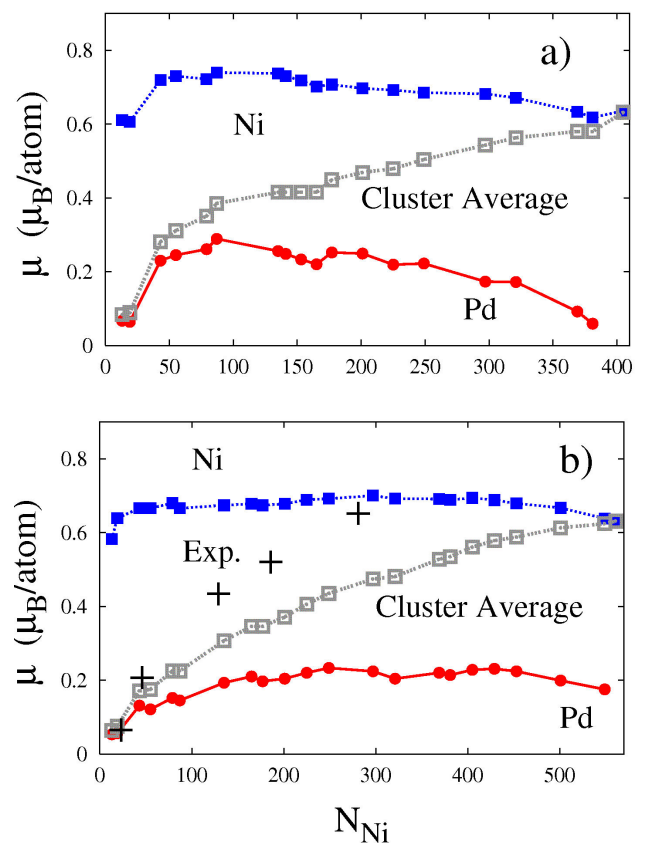


FIGURE 2. Magnetic moment per atom as a function of the number of Ni atoms for different cluster sizes with cubo-octahedral structure in the full segregated configuration (Ni cores coated by Pd atoms), a) corresponds to $N = 405$ atoms in the truncated cubo-octahedron structure, and b) to $N = 561$ in the octahedron structure. \square corresponds to average cluster magnetic moments, \blacksquare to average Ni magnetic moments, and \bullet to average Pd magnetic moments. We also show the experimental results (crosses) by Nuno-mura [9] for 562 atom NiPd clusters.

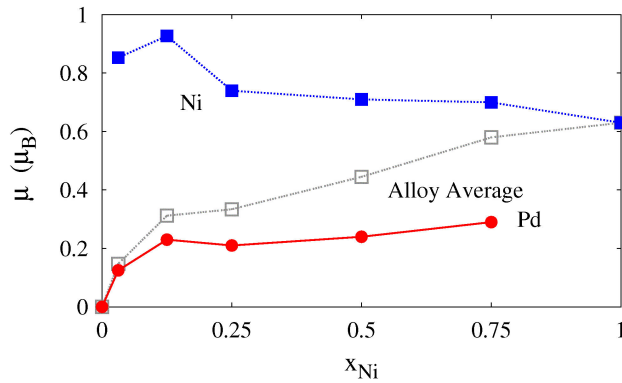


FIGURE 3. *Ab initio* magnetic moment per atom as a function of Ni concentration for fcc $\text{Ni}_x\text{Pd}_{1-x}$ ordered bulk alloys.

information on cluster structure or on chemical order is given, although the icosahedral structure has been suggested in the experimental report.

It is worth comparing the magnetic moments calculated for the clusters with those obtained for bulk alloys, theoretical and experimentally [28]. With this aim, we perform additional *ab initio* calculations [21] for different ordered NiPd fcc-bulk alloys. In these calculations we consider an $L1_0$ structure for $x = 1/2$, an $L1_2$ for $x = 1/4$ and $3/4$, and for $x = 1/8$ ($1/32$) we take into account a double (octuple) $L1_2$ structure with 8 (32) atoms in the unit cell and in which a single Ni atom is placed at the origin. In Fig. 3, it can be clearly seen that bulk alloys show a behavior similar to the clusters as a function of Ni concentration and agree well with the experimental results. In this case no low-dimensional effects are present.

Now, let us consider a case in which the hardness of the magnetic moment of the $3d$ component is greater than that of Ni, that is we replace Ni atoms by Co ones. In Fig. 4, we show the results obtained for the average magnetic moment per atom as a function of Co content (N_{Co}) for core/shell clusters with the same configurations as those of Fig. 2b but considering $N = 147, 309$, and 561 . In both cases, NiPd and CoPd clusters, the average magnetic moment of the Pd atoms as a function of the $3d$ core size is similar. A large enhancement of the magnetic moment of Co is mainly observed in the low concentration region as depicted in Fig. 2. In this figure, the upper nearly-constant curve gives the average Co magnetic moment as a function of Co content, the lower curve gives the corresponding values for Pd, while the one in between (open squares) gives the total average magnetic moment per atom in the system. As in the previous case, the enhancement in the magnetic moment of Co, as compared to the bulk value, is due to finite size effects and to hybridization with the Pd atoms as well. Although in general the results are similar, it is worth noticing that in the very dilute limit the Co atoms show a larger enhancement of the magnetic moments than in the case of Ni. When we have only one Co atom in the core, we are in the presence of a magnetic impurity; this explains the large local moment obtained as shown in Fig. 4. For the three different cluster sizes (for $N = 147, 309$, and

561), the obtained value of $2.2\mu_B$ for Co agrees with previous theoretical ones of $2.28\mu_B$ [24] and with experimental results ($2.1 \pm 0.3\mu_B$ [25]). The average magnetic moment per Co atom tends towards the free standing cluster value as a function of Co concentration (without taking into account the orbital contribution), with $\mu_{\text{Co}} = 1.66\mu_B$ for the three different sizes considered in agreement with the experimental reports of $\mu_{\text{Co}_N} = (2.00 \pm 0.03)\mu_B$, $(1.84 \pm 0.05)\mu_B$, and $(1.74 \pm 0.05)\mu_B$ for $N = 147, 309$, and 561 , respectively [26].

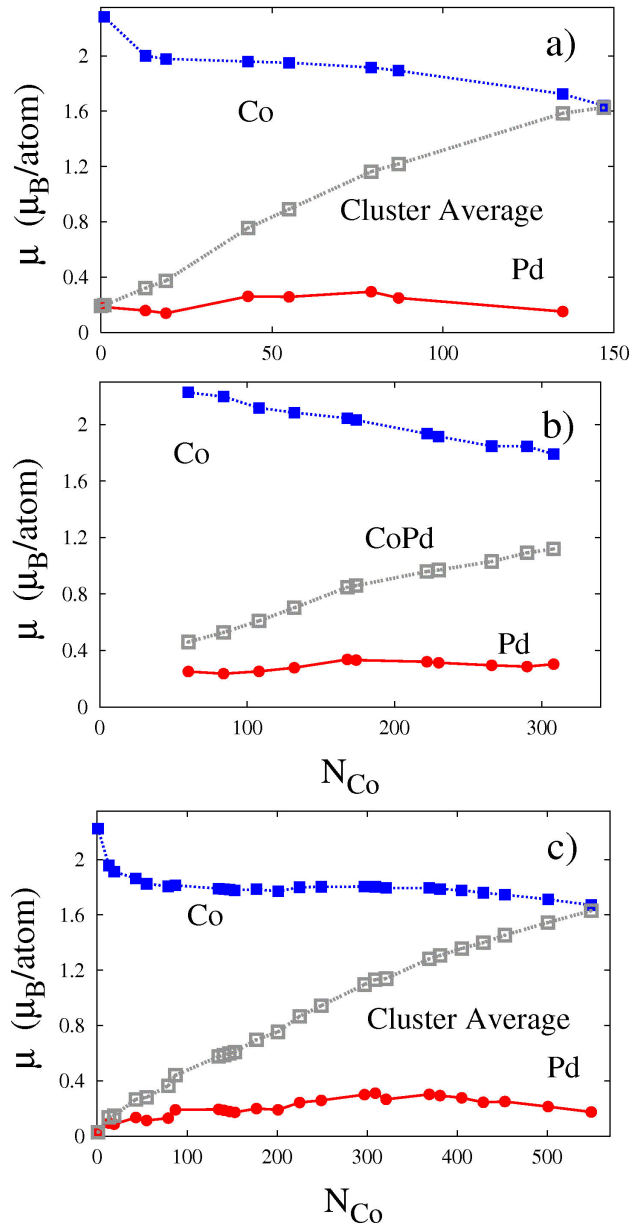


FIGURE 4. Magnetic moment per atom as a function of the number of Co atoms for the segregated configurations (Co cores coated by Pd). The total number of atoms in the cluster is a) 147, b) 309, and c) 561 in a cubo-octahedral structure.

2.2. Onion-like Cluster calculations

With the aim of finding the dependence of the magnetic properties on chemical order, we perform additional calculations considering A/B/A onion-like arrangements [14] (Pd core/ Ni or Co subsurface/ Pd surface) for 561 atom clusters with cubo-octahedral structure and a fixed number of Pd atoms at the surface (252 atoms). This structure presents a core of 309 atoms and a surface region of 252 atoms. The onion-like structure is given by $\text{Pd}_{309-N}/\text{Ni}_N/\text{Pd}_{252}$ with N going from 60 to 309. The $N = 309$ case corresponds to $N_{\text{Ni}} = 309$ in Fig. 2b. In Fig. 5a and 5b we show the results for $\text{Pd}_{309-N}/\text{Ni}_N/\text{Pd}_{252}$ and $\text{Pd}_{309-N}/\text{Co}_N/\text{Pd}_{252}$, respectively. Both graphs show similar tendencies, although at low concentrations the CoPd clusters show a larger enhancement of the Co magnetic moments while in NiPd clusters the magnetic moment of Ni is almost constant. It is worth noticing that larger values of the average magnetic moments are observed in the onion-like structures than in the core/shell ones, due to the fact that a larger number of NiPd and CoPd bonds are present in this case. In Fig. 5a we also include experimental results (crosses) [9]. It can be seen that a better agreement with the experiments is obtained than in Fig. 2b. This suggests that experimentally the systems probably present an onion-like configuration. This A/B/A order is theoretically suggested for binary cubo-octahedral structures even if for highly segregated systems it is more likely to be observed for icosahedral than for cubo-octahedral structures [14].

2.3. Thin film Calculations

We compare the results of NiPd and CoPd clusters with nanostructures of higher dimensionality. We calculate the electronic properties of 7-layer slabs. In Fig. 6 we schematically show three different arrangements for CoPd slabs with $x_{\text{Co}} = 2/7$. We consider in this case not only Pd-coated Ni or Co thin films but also arrangements in which Pd lies in central layers (onion-like). In Fig. 7 we show the results for the magnetic moments as a function of Ni or Co concentration, x_{Ni} or x_{Co} respectively. For each concentration different arrangements are considered and the full line goes through those of minimum energy. It can be clearly seen that the slab results show a behavior similar to the cluster ones. For $x_{\text{TM}} = 1/7$, and $= 6/7$ we have just one configuration (3Pd/TM/3Pd and 3TM/Pd/3TM respectively), for $x_{\text{TM}} = 2/7, 3/7, 4/7$, and $5/7$ three different layered arrangements are studied. The $x_{\text{TM}} = 2/7$ ones are schematically shown in Fig. 6.

The pure Pd 7-layer slab shows no magnetization in agreement with previous semi-empirical theoretical calculations performed by Bouarab [29]. The pure Ni and Co 7-layer slabs present a slightly higher average magnetic moment than their bulk values ($\mu_{\text{Ni}} = 0.59\mu_B$ and $\mu_{\text{Co}} = 1.53\mu_B$). On the other hand, at low Ni and Co concentration regions we can clearly see that Ni and Co reach magnetic values close to $0.87\mu_B$ and $1.98\mu_B$ in agreement with the impurity limit

case as quoted above. In the neighborhood of the equi-atomic region, the magnetic moment values of the thin films for $3/7 < x_{\text{TM}} < 4/7$ are congruent with previous theoretical

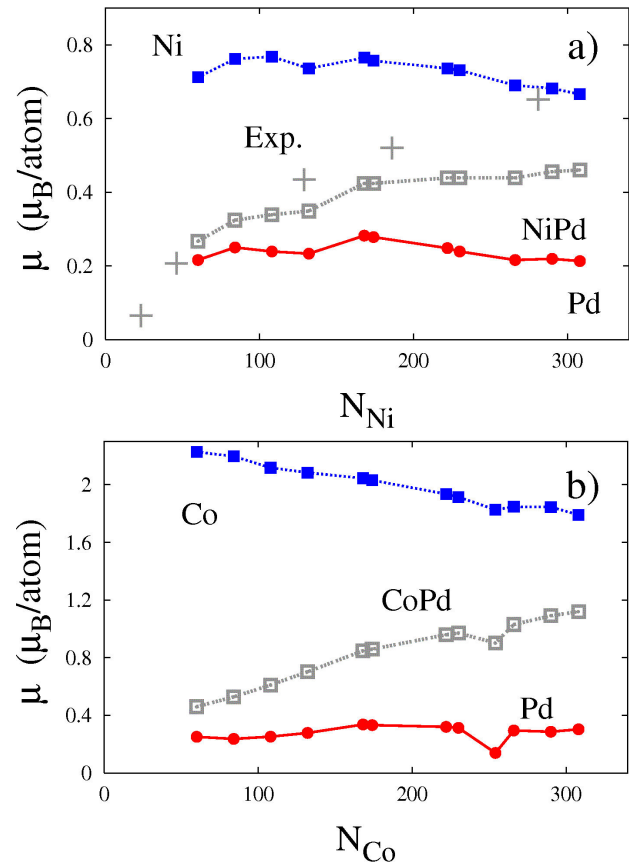
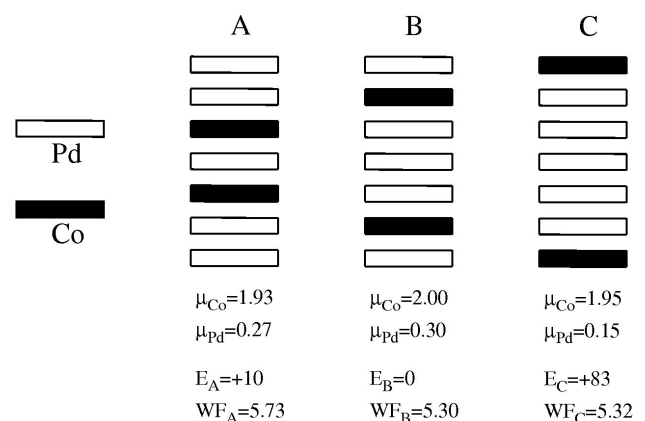


FIGURE 5. Magnetic moment per atom as a function of the number of a) Ni atoms and b) Co atoms, for onion-like structures (Pd-core/Ni-shell/Pd-252). The total number of atoms in the clusters is 561 in a cubo-octahedral structure. We also show the experimental results (crosses) by Nunomura [9] for 562 atom NiPd clusters.



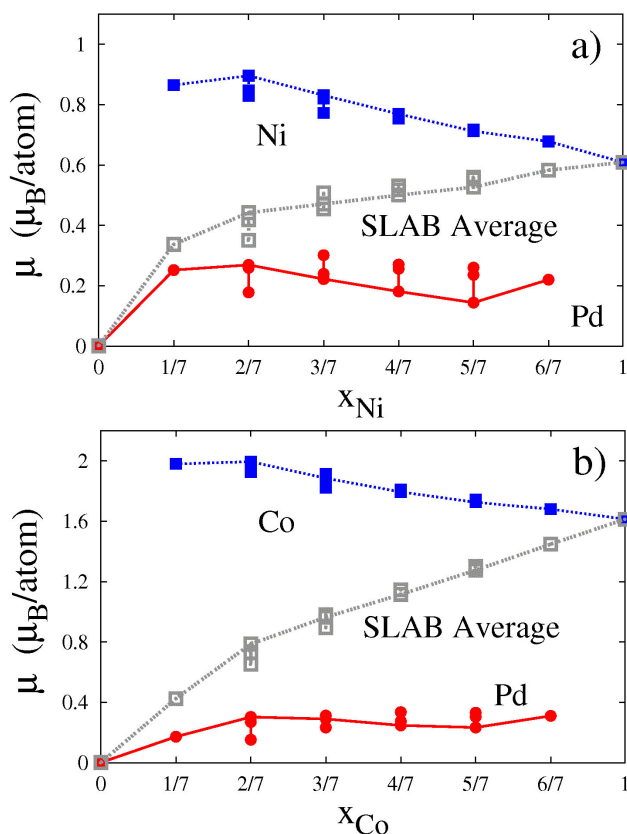


FIGURE 7. Magnetic moments per atom as a function of a) Ni and b) Co concentration, for 7 layer NiPd and CoPd fcc-slabs, respectively, grown in the (111) direction obtained by *ab-initio* calculations. The solid line corresponds to the minimum energy arrangements.

and experimental results for $L1_0$ bulk alloy systems [30]. It is worth noticing that in the case of $x_{\text{TM}} = 2/7, 4/7, \text{ and } 6/7$, the central layer is always made of Pd. Except for $x_{\text{TM}} = 6/7$, whose unique configuration presents the Pd layer in the middle of the slab, all the others have at least one arrangement with the Pd atoms at the surface. These are the minimum energy configurations; we find that Ni and Co layers prefer to sit at the sub-surface positions.

In the case of the CoPd slabs, for $x_{\text{Co}} = 2/7$ we consider three different layer arrangements (see Fig. 6). For $2\text{Pd}/\text{Co}/\text{Pd}/\text{Co}/2\text{Pd}$ ("A" in Fig. 6) we obtain the lowest value for the magnetic moment of Co, namely $\mu_{\text{Co}} = 1.93\mu_B$, while $\mu_{\text{Pd}} = 0.27\mu_B$. In the case of the slab $\text{Co}/5\text{Pd}/\text{Co}$, the Co atoms are at the surface ("C" in Fig. 6), and we obtain $\mu_{\text{Co}} = 1.95\mu_B$ and $\mu_{\text{Pd}} = 0.15\mu_B$. We have a similar magnetization for Co as in the previous case but, on the other hand, a lower Pd magnetization (Pd is not at the surface). The most interesting case is the one with the Co atoms in the sub-surface layer, $\text{Pd}/\text{Co}/3\text{Pd}/\text{Co}/\text{Pd}$, ("B" in Fig. 6). In this case $\mu_{\text{Co}} = 2.00\mu_B$ and $\mu_{\text{Pd}} = 0.30\mu_B$; both hybridization and surface effects, contribute to the enhancement of the magnetic moment of Co and Pd atoms. Among the three arrangements considered here, this is the one with the lowest

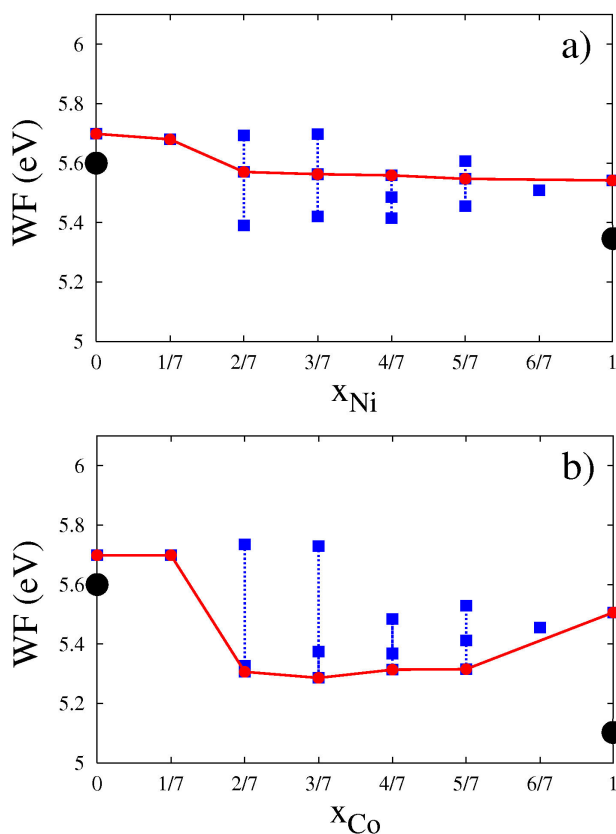


FIGURE 8. Work function as a function of a) Ni and b) Co concentration for the 7 layer NiPd and CoPd fcc-slabs, respectively, grown in the (111) direction obtained by *ab-initio* calculations. Bullets indicate the corresponding experimental bulk values. The solid line corresponds to the minimum energy arrangements.

total energy. These results show the importance of the local environment (surface effects and hybridization) on the magnetic properties of $3d$ - $4d$ slab systems.

A relevant electronic property in catalysis is the Work Function (WF). This is a size-dependent property that increases as the system size decreases. In bulk the energy required to add or remove an electron is the WF. In Fig. 8 we show the WF, calculated as a function of TM concentration for the slabs of Fig. 7. In Fig. 8a we present the NiPd slab values. The two bullets correspond to experimental values taken on the (111) surfaces [31]. We can point out that the differences among the slabs' and bulks' WF are mainly due to size effects and that the slab values are, as expected, higher than the bulk ones. The solid line corresponds to the minimum energy arrangements. It can be seen that there is a smooth dependence of the WF on x_{Ni} .

In Fig. 8b we show the corresponding CoPd slab WF values and the two bullets correspond to bulk experimental values. It is evident that for this system the WF presents a strong decrease at $x_{\text{Co}} = 2/7$, even lower than for the 7-layer Co slab. The necessary energy to take off an electron from the CoPd slabs with $2/7 < x_{\text{Co}} < 5/7$ is lower than for the pure Pd and Co slabs. These systems show large fluctuations in the WF values as a function of the different arrangements

considered for a fixed concentration. The WF is then a very sensitive property, depending strongly on chemical order.

We also calculate the magnetic moment and Work Function as functions of concentration of NiPd and CoPd slabs grown in the (100) and (110) direction. They present similar tendencies as shown in Figs. 7 and 8. In all cases the arrangements with Pd at surface sites are those with minimum energy. There is no tendency of segregation of the Ni atoms to the (111) surface at any concentration [32].

3. Conclusions

In summary, we study the magnetic behavior of segregated NiPd and CoPd nanoclusters as a function of the $3d$ -atom concentration and show that hybridization is the main reason for the enhancement of the average magnetic moment of $3d$ and Pd atoms within the clusters, although surface effects also play an important role. We find that the values of the magnetic moments at the different concentrations are very similar to those obtained for bulk alloys by doing *ab initio* calculations, even if the magnetic moment of the Ni and Co atoms are larger in the onion-like structures than in the core/shell ones. In particular the Pd magnetic moments lie around $0.2\mu_B$, both in bulk alloys as well as in Pd-coated clusters for the NiPd systems, and are slightly higher for CoPd systems. This polarization is the maximum attainable by Pd and can be triggered both by surface as well as by hybridization effects. The enhancement due to hybridization is reflected in the values obtained for onion-like clusters.

The pure Ni and Co clusters and slabs have the maximum average magnetic moment value per atom. When adding Pd

atoms to the system, these average values begin to decrease because the polarization of the Pd atoms is not high. However, on the contrary, the Ni and Co magnetic moments begin to enhance, particularly in the case of Co-Pd systems. We attribute this enhancement to the Co- and Ni-Pd hybridization. This enhancement due to hybridization is even more clearly reflected in the values obtained for onion-like clusters.

The thin films studied show that the magnetic moments as a function of concentration have similar tendencies as for the clusters. Ni and Co atoms have higher magnetic moments in sub-surface sites than in surface ones. The Work Function of CoPd thin films shows a stronger dependence on Co concentration than the NiPd ones on the corresponding Ni concentration, reaching even lower values than those of pure Pd and Co slabs.

Acknowledgments

Javier Guevara and Ana María Llois are also researchers of CONICET. We acknowledge PICT 03-10698 of Agencia Nacional de Promoción Científica y Tecnológica, PIP 6016 of CONICET, Grant SA06/070 of UNSAM, for partial support. This work was partially funded by the PROMEP-SEP-CA-16-2007-24-21, México. Also JMMC and FAG acknowledge the financial support from CONACyT (México) through grants No. 50650. Computer resources from the Centro Nacional de Supercomputo (CNS) from the Instituto Potosino de Investigación Científica y Tecnológica (IPICYT), San Luis Potosí, México, is also acknowledged. We also wish to thank J. Limón-Castillo for computational assistance.

-
1. D. Zitoun *et al.*, *Phys. Rev. Lett.* **89** (2002) 037203.
 2. S. Dennler, J. Morillo, and G. Pastor, *Surf. Sci.* **532-535** (2003) 334.
 3. E.O. Berlanga-Ramírez *et al.*, *Phys. Rev. B* **70** (2004) 014410.
 4. T. Sondón and J. Guevara, *J. Mag. Mag. Mat.* **272-276** (2004) e1247.
 5. J. Guevara, A.M. Llois, and M. Weissmann, *Phys. Rev. Lett.* **81** (1998) 5306.
 6. X. Chuanyun, Y. Jinlong, D. Kaiming, and W. Kelin, *Phys. Rev. B* **55** (1997) 3677.
 7. Y. Xie and John A. Blackman, *Phys. Rev. B* **66** (2002) 155417.
 8. N. Nunomura, H. Hori, T. Teranishi, M. Miyake, and S. Yamada, *Phys. Lett. A* **249** (1998) 524.
 9. N. Nunomura *et al.*, *Jour. Mag. Mag. Mat.* **177-181** (1998) 947; H. Hori *et al.*, *Physica B* **294-295** (2001) 292.
 10. J-M. Roussel, A. Saúl, G. Tréglia, and B. Legrand, *Phys. Rev. B* **69** (2004) 115406.
 11. C. Mottet, G. Tréglia, and B. Legrand, *Phys. Rev. B* **66** (2002) 045413.
 12. S. Sao-Joao *et al.*, *J. Phys. Chem. B* **109** (2005) 342.
 13. A.V. Ruban, H.L. Skriver, and J.K. Nørskov, *Phys. Rev. B* **59** (1999) 15990.
 14. F. Baletto, C. Mottet, and R. Ferrando, *Phys. Rev. Lett.* **90** (2003) 135504.
 15. P. Villaseñor-González, R. Guirado-López, J. Dorantes-Dávila, and G.M. Pastor, *European Physical Journal D* **24** (2003) 73.
 16. Q. Wang, Q. Sun, J.Z. Yu, Y. Hashi, and Y. Kawazoe, *Phys. Lett. A* **267** (2000) 394.
 17. J. Guevara, F. Parisi, A.M. Llois, and M. Weissmann, *Phys. Rev. B* **55** (1997) 13283.
 18. O.K. Andersen and O. Jepsen, *Phys. Rev. Lett.* **53** (1984) 2471; O.K. Andersen, O. Jepsen, and D. Gloetzel, in *Highlights of Condensed Matter Theory*, edited by F. Bassani, F. Fumi, and M. Tosi (North Holland, Amsterdam, 1985)
 19. T. Bandyopadhyay and D.D. Sarma, *Phys. Rev. B* **39** (1989) 3517.
 20. J.F. Janak, *Phys. Rev. B* **16** (1977) 255.

21. P. Blaha, K. Schwarz, G.K.H. Madsen, D. Kvasnicka, and J. Luitz, *WIEN2k, an augmented plane wave + local orbitals program for calculating crystal properties*, Karlheinz Schwarz, Techn. Universität Wien, Austria, 2001, ISBN 3-9501031-1-2; P. Blaha, K. Schwarz, P. Sorantin, and S.B. Trickey, *Comput. Phys. Comm.* **59** (1990) 399.
22. A.T. Aldred *et al.*, *Phys. Rev. Lett.* **24** (1970) 897.
23. W. Loram *et al.*, *J. Phys. F* **15** (1985) 2213.
24. A. Oswald, R. Zeller, and P.H. Dederichs, *Phys. Rev. Lett.* **56** (1986) 1419.
25. G.G. Low and T.M. Holden, *Proc. Phys. Soc. London* **89** (1966) 119.
26. I.M.L. Billas, A. Châtelain, and W.A. de Heer, *Science* **265** (1994) 1682.
27. S.E. Apsel, J.W. Emmert, J. Deng, and L.A. Bloomfield, *Phys. Rev. Lett.* **76** (1996) 1441.
28. J.W. Cable and H.R. Child, *Phys. Rev. B* **1** (1970) 3809.
29. S. Bouarab, C. Demangeat, A. Mokrani and H. Dreyseé, *Phys. Lett. A* **151** (1990) 103; S. Bouarab, H. Nati-Laziz, C. Demangeat, A. Mokrani, and H. Dreyseé, *J. Magn. Magn. Mater.* **104-107** (1992) 1765.
30. P.M. Oppeneer, *Handbook of Magnetic Materials* (North Holland, 2001) Vol. 13, p. 229.
31. *Cohesion in Metals*, editors F.R. de Boer, R. Boom, W.C.M. Mattens, A.R. Miedema, and A.K. Niessen (North-Holland, 1988).
32. L.V. Pourovskii, A.V. Ruban, I.A. Abrikosov, Y.Kh. Vekilov, and B. Johansson, *Phys. Rev. B* **64** (2001) 035421.